JOURNAL OF APPLIED ELECTROCHEMISTRY 19 (1989) 83–89

Chemical and electrochemical inhibition studies of corrosion and hydrogen surface embrittlement. I. $Fe_{0.78}B_{0.13}Si_{0.09}$ amorphous alloy in molar HCl

S. KERTIT, J. ARIDE

Ecole Normale Supérieure (Takaddoum), Rabat, Morocco

A. BEN-BACHIR, A. SGHIRI

Department of Chemistry, Faculty of Sciences, Rabat, Morocco

A. ELKHOLY, M. ETMAN

Laboratoire d'Electrochimie Interfaciale du C.N.R.S., 1, Place A. Briand, 92195 Meudon Principal Cédex, France

Received 15 March 1988; revised 14 July 1988

Diorthoaminophenoldisulfane (DOAPD) was synthesized for use as a corrosion inhibitor and in order to test its effect on the hydrogen surface embrittlement of $Fe_{0.78}B_{0.13}Si_{0.09}$ alloy. Results of electrochemical and gravimetric measurements were consistent and confirmed the beneficial role of this inhibitor. The amorphous state of the alloy was confirmed by X-ray measurements and differential thermal analysis. The maximum inhibition of corrosion was attained in the presence of 10^{-4} M DOAPD. This inhibitor concentration also gave rise to a diminution of metal hydrogenation. A mechanism explaining the mixed role of the disulfane was confirmed.

1. Introduction

Amorphous alloys, prepared by high speed quenching techniques, are generally regarded as interesting and important new metallic materials. The magnetic, electric, mechanical and chemical properties of such alloys [1–11] are attractive and are the reason for their potential applications. In the literature it has been shown that some metallic amorphous alloys are highly resistant to corrosion and hydrogen embrittlement [12–14]. Initially, this property was attributed to the absence of the characteristic structural defects of crystalline phases. Subsequently, some authors showed that the chemical composition of amorphous alloys plays a major role in the improvement of their corrosion resistance [15–17]. It is usually admitted that the iron metalloid amorphous alloys containing no other metallic element have a weak resistance for corrosion and hydrogen embrittlement [18–20]. Other authors noted that the amorphous alloys $Fe_{0.75}B_{0.25-x}Si_x$ have a weak corrosion resistance when x is smaller than 0.12 [21]. Also, an absence of passivity was shown in buffered borate solutions.

It is important to note that the possible improvement of the resistance to corrosion and hydrogen embrittlement of some amorphous alloys by addition of an inhibitor compound in an aggressive medium has not been studied previously. The organic inhibitor diorthoaminophenoldisulfane used for this work was synthesized as described elsewhere [22, 23]. This compound was used successfully as an inhibitor of corrosion and hydrogen surface embrittlement for crystalline α-Fe in 1 M HCl [22, 23]. This compound did not show any inhibition in H_2SO_4 for crystalline α-Fe. This was the reason why we limited our studies to the inhibiting effect on the amorphous alloy $Fe_{0.78}B_{0.13}Si_{0.09}$ in 1 M HCl. To our knowledge this is the first time that DOAPD has been used as an inhibitor for corrosion and hydrogen surface embrittlement of an amorphous alloy in aggressive media.

2. Experimental details

The amorphous alloy used in this work was prepared at the research center of 'Pont à Mousson' by the high speed quenching technique (melt-spinning). In the form of a tape, the side in contact with the cylinder, necessary for the elaboration of the amorphous alloy [24], is matt while the reverse side is bright. The dimensions of the tape were: length = 100 cm, width = 1 cm, thickness = 40 μm.

2.1. *Electrochemical measurements*

Electrochemical studies were carried out in a double-walled Pyrex glass three-electrode electrolysis cell containing the aggressive medium and thermostated at 19 ± 1° C. The disc working electrode was cut from the amorphous tape and pressed onto a hollow steel support filled with a chemically inert resin. The

0021-891X/89 $03.00 + .12

electrolyte (HCl) was deaerated for 1 h using argon prior to the experiment. The apparent surface of the working electrode was 0.65 cm^2. Electrode potentials were measured with respect to a saturated calomel electrode (SCE). The surface of the platinum counter electrode was larger than that of the working electrode. The working electrode was pre-treated by cleaning with acetone, followed by washing with bidistilled water and drying in an inert gas or eventually in air.

The amorphous disc electrode was polarized at −800 mV/SCE for 15 min before recording the potentiodynamic curves. The applied potential was then increased.

The working electrode was loaded with hydrogen by cathodic polarization at −1500 mV/SCE for 30 min in 1 M HCl either in the absence or in the presence of the inhibitor DOAPD. It is important to note that the previous electrochemical measurements were carried out on the bright side of the working amorphous alloy electrode. The scanning rate 0.5 mV s^{-1} was chosen in order to approximate to stationary conditions.

2.2. *Gravimetric measurements*

Experiments were carried out in a double-walled Pyrex glass cell equipped with a thermostated cooling condenser. The solution volume was 100 cm^3. The amorphous specimens used had a rectangular form (length = 4 cm; width = 1 cm; thickness = 40 μm).

3. The inhibitor

The choice of the inhibitor DOAPD was based on: (i) the high availability of the free electron pairs on the sulfur atoms which ensure anodic inhibition characteristics [25, 26]; (ii) the amino groups which give cathodic inhibition characteristics [27, 28]. Additionally, interactions between the π electrons of the aromatic nuclei and the d orbitals of the metal may also inhibit metal dissolution [29, 30].

DOAPD has a large molecular surface area which assures a good covering of the metallic surface. The inhibitor was prepared by condensation of 2-aminothiophenol in the presence of air at room temperature according to the following reaction [22, 23]:

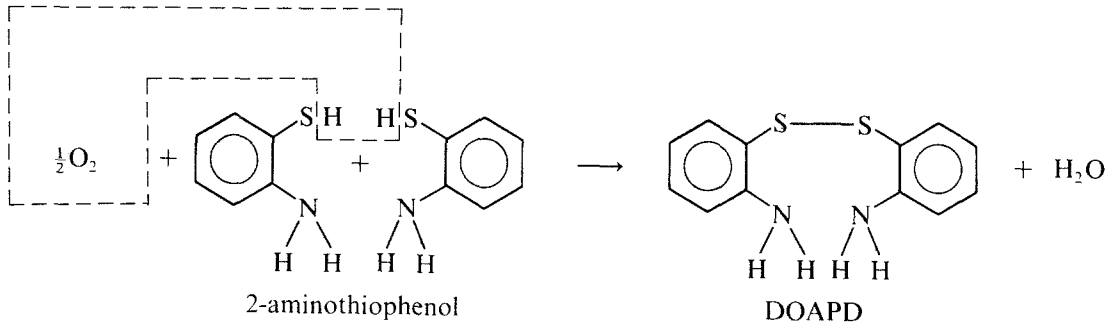

It was difficult to differentiate between 2-aminothiophenol and the resulting product by elementary weight analysis. However, the composition of the product (DOAPD with chemical formula $C_{12}H_{12}N_2S_2$ and fusion point 78° C) was identified and confirmed by analytical NMR, IR and mass spectroscopy [22, 23]. This analysis showed clearly the absence of 2-aminothiophenol.

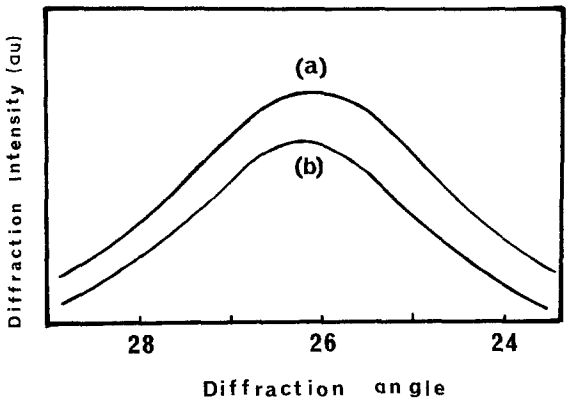

Fig. 1. X-ray diffraction response of the $Fe_{0.78}B_{0.13}Si_{0.09}$ amorphous alloy: (a) bright side; (b) matt side.

4. Characterization of the alloy

The atomic composition of the studied alloy is $Fe_{0.78}B_{0.13}Si_{0.09}$ and its amorphous structure was confirmed by X-ray diffraction and differential thermal analysis. The X-ray diffraction results (Fig. 1) obtained from the two sides of the alloy showed only a diffuse halo, characteristic of the amorphous state. No traces of crystallization were detected on either side.

From the thermograph obtained by differential thermal analysis of the alloy (Fig. 2) at 10° C min^{-1}, this alloy crystallizes in two steps as shown by the two peaks of crystallization at 545° C and 560° C.

5. Experimental results and discussion

5.1. *Electrochemical results*

5.1.1. Comparative study of the amorphous $Fe_{0.78}B_{0.13}S_{0.09}$ alloy and crystalline iron. In Fig. 3 are compared the potentiodynamic curves of the amorphous alloy $Fe_{0.78}B_{0.13}S_{0.09}$ and crystalline α-iron in 1 M HCl. The anodic current of the amorphous alloy increases sharply starting at its corrosion potential, a typical characteristic of very weakly corrosion-resistant solids. Corrosion current densities were determined for both samples by the extrapolation of the cathodic Tafel lines to the corrosion potential.

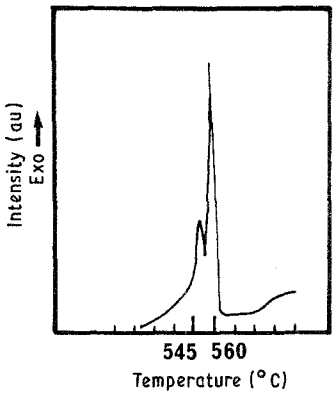

Fig. 2. Diagram of differential thermal analysis of the $Fe_{0.78}B_{0.13}Si_{0.09}$ alloy. Rate of temperature rise is $10°C\,min^{-1}$.

The corrosion current density of the amorph, $300\,\mu A\,cm^{-2}$, is higher than that of crystalline α-iron ($150\,\mu A\,cm^{-2}$).

The corrosion potential of iron is slightly more positive than that of the amorphous alloy. We can therefore conclude that this amorphous alloy is less corrosion resistant than crystalline α-iron in 1 M HCl.

5.1.2. Effect of inhibitor concentration. The potentiokinetic polarization curves of the amorphous alloy were recorded in 1 M HCl, and are shown in Fig. 4 for a range of inhibitor concentrations. A decrease in both cathodic and anodic currents is noted. The variation of the free corrosion potential of the amorphous alloy with inhibitor concentration in 1 M HCl is illustrated in Fig. 5. The corrosion potential shifts to more positive values with increasing inhibition concentration. The curves in Figs 4 and 5 can be explained as follows. Initially, the aqueous solution contains free

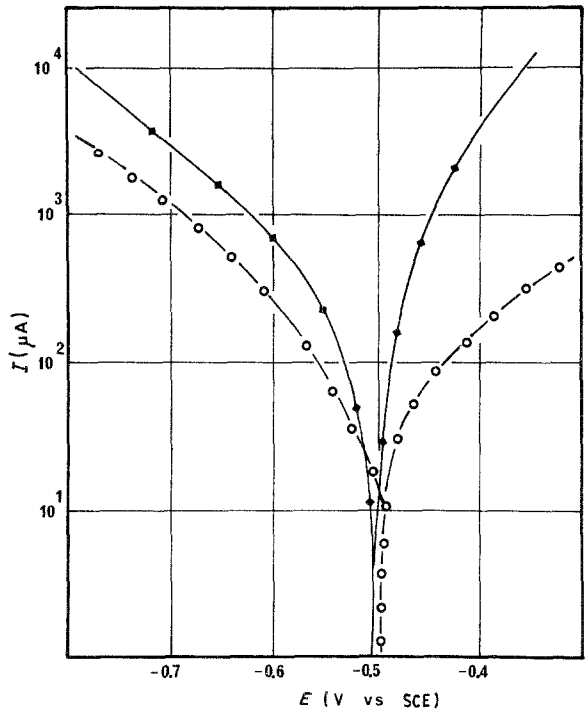

Fig. 3. Potentiokinetic polarization curves of: (○) α-crystalline iron and (■) amorphous $Fe_{0.78}B_{0.13}Si_{0.09}$ alloy in 1 M HCl. Working electrode surface area is $0.65\,cm^2$.

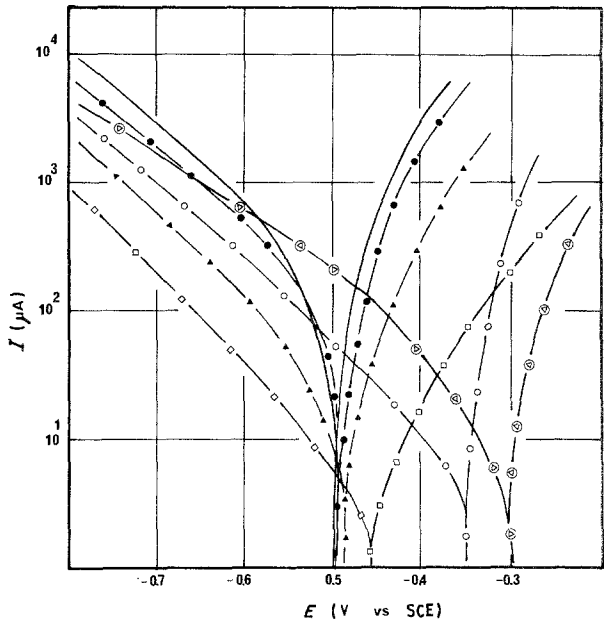

Fig. 4. Potentiokinetic polarization curves of $Fe_{0.78}B_{0.13}Si_{0.09}$ alloy in 1 M HCl in the presence of different concentrations of DOAPD inhibitor. —— 0.0; (●) 10^{-6}; (▲) 10^{-5}; (□) 10^{-4}; (○) 10^{-3}; (◎) 5×10^{-3} M. Working electrode surface area is $0.65\,cm^2$.

solvated cations and anions. In the cathodic potential region the inhibitor bulk preferentially reacts with protons giving $^{+}H_3N\text{-}C_6\text{-}H_4\text{-}S\text{-}S\text{-}C_6\text{-}H_4\text{-}NH_3^{+}$, while in the anodic potential region where Cl^- anions predominate near the electrode surface, DOAPD is adsorbed at the surface due to the free electron pairs on the sulfur atoms as well as the π electrons of the aromatic rings. This mechanism supposes that the formula of the ionic adsorbed species is $(S\text{-}C_6H_4\text{-}NH_3^{+}\,Cl)_2$ and these ions replace adsorbed Cl^- ions in the anodic region. The apparent protection of the amorphous surface in this acid medium may be explained as follows. If it is assumed that Cl^- anions are first adsorbed onto the amorphous surface, the adsorption of the cationic bulk species $(S\text{-}C_6H_4\text{-}NH_3^{+})_2$ would be limited by the surface concentration of Cl^-, the cationic species being adsorbed

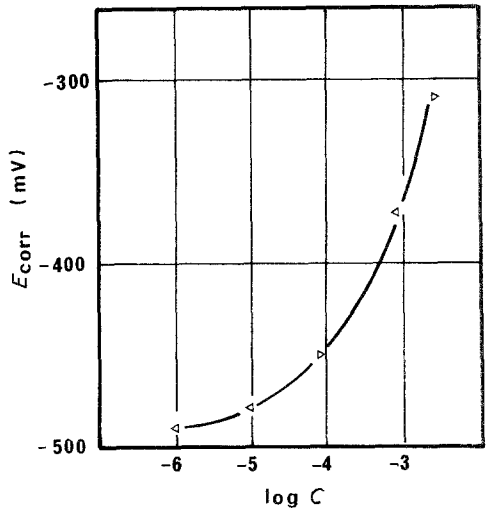

Fig. 5. Corrosion potentials of the $Fe_{0.78}B_{0.13}Si_{0.09}$ alloy as a function of DOAPD concentration in 1 M HCl.

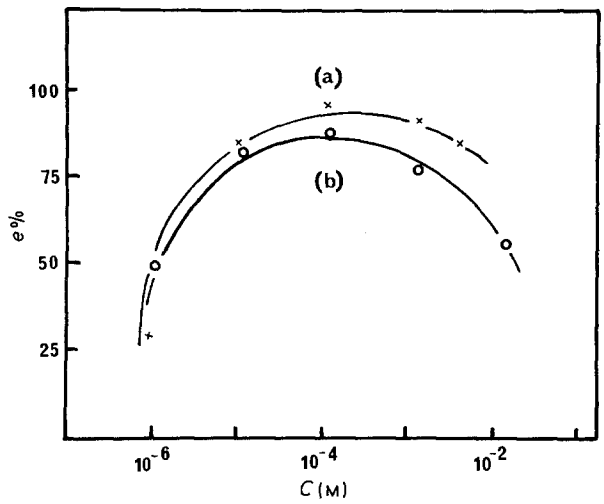

Fig. 6. Inhibition efficiency of corrosion of $Fe_{0.78}B_{0.13}Si_{0.09}$ in 1 M HCl as a function of concentration of DOAPD: (a) electrochemical results; (b) gravimetric results.

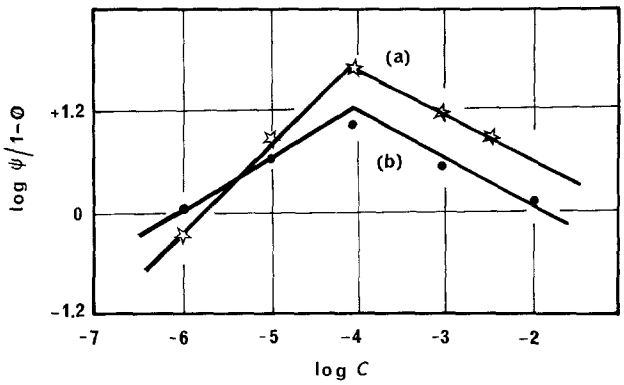

Fig. 7. Indirect Langmuir isotherm adsorption model of DOAPD of concentration up to 10^{-4} M on the surface of $Fe_{0.78}B_{0.13}Si_{0.09}$ alloy in 1 M HCl: (a) electrochemical results; (b) gravimetric results.

when possible on free surface sites. This is similar to the mechanism proposed for mercury by Bockris and Blomgren [30]. Alternatively, the $(S\text{-}C_6\text{-}H_4NH_3^+)_2$ may link with $2Cl^-$ on the surface to form a neutral species bound by Cl-surface and S-surface interactions. The characteristics of the rate of the corrosion process were determined by the corrosion current density (i_C) calculated from the extrapolation of the Tafel curve to the corrosion potential (E_C) of the working electrode.

Consequently we can calculate the inhibition efficiency (e%) as defined by the classical expression:

$$e = \frac{(i - i')}{i} \times 100$$

where i' and i represent corrosion current densities of the treated alloy with and without inhibitor.

Values of corrosion current densities, corrosion potentials and corrosion inhibition efficiencies for each inhibitor concentration studied are given in Table 1.

The effect of DOAPD on the corrosion inhibition of the amorphous alloy in 1 M HCl for each inhibitor concentration is shown in Fig. 6a.

We note that the inhibition efficiency increases with inhibitor concentration and attains a maximum (critical) value of 98% at 10^{-4} M DOAPD. Inhibitor concentrations higher than 10^{-4} M lead to a decrease of inhibitor efficiency.

The fraction of surface covered, θ, was expressed by the ratio $(i - i')/i$ where i' and i are current densities in the presence and absence of the DOAPD.

The relation between $\log \theta/1 - \theta$ and $\log C$, where C is the inhibitor concentration, is linear up to 10^{-4} M as shown in Fig. 7. Thus, at low concentrations, where the Langmuir approximation is valid, the indirect adsorption of DOAPD corresponds to a Langmuir isotherm where $\theta/1 - \theta = kC \exp(q/RT)$. q = heat of adsorption, $k = ct$, C = inhibitor concentration. This indirect absorption of the ionized form of the inhibitor is controlled by the concentration of Cl^- anions and depends on the free sites after the liberation of the Cl^- as discussed earlier.

This isotherm can be used because of the surface homogeneity of the amorphous alloy. For crystalline α-iron, which displays surface heterogeneity, the indirect adsorption of DOAPD has been shown to correspond to the Temkin isotherm [31].

DOAPD is therefore a mixed inhibitor, inhibiting hydrogen evolution on the amorphous surface and the anodic dissolution of the metal.

6. Gravimetric results

Efforts were also made to study by a chemical method the behaviour of this amorphous alloy under the same experimental conditions. 100 ± 10 mg of alloy was

Table 1. Corrosion potentials, corrosion current densities and inhibitor efficiency 'e' as a function of molar concentrations of DOAPD inhibitor added to 1 M HCl electrolyte

Concentration of DOAPD inhibitor	E_{corr} (mV)	I_{corr} ($\mu A\,cm^{-2}$)	*Inhibitor efficiency* (%)
0	−500	300	–
10^{-6}	−494	220	26
10^{-5}	−485	25	87
10^{-4}	−455	6	98
10^{-3}	−350	17	94
5×10^{-3}	−300	36	88

Table 2. Weight loss of $Fe_{0.78}B_{0.13}Si_{0.09}$ amorphous alloy as a function of DOAPD molar concentrations added to 1 M HCl. Calculated inhibitor efficiency 'e' produced

Concentration of DOAPD inhibitor	w ($mg\,cm^{-2}\,h^{-1}$)	*Inhibitor efficiency* (%)
0	0.5	–
10^{-6}	0.25	50
10^{-5}	0.07	86
10^{-4}	0.05	90
10^{-3}	0.1	80
10^{-2}	0.22	56

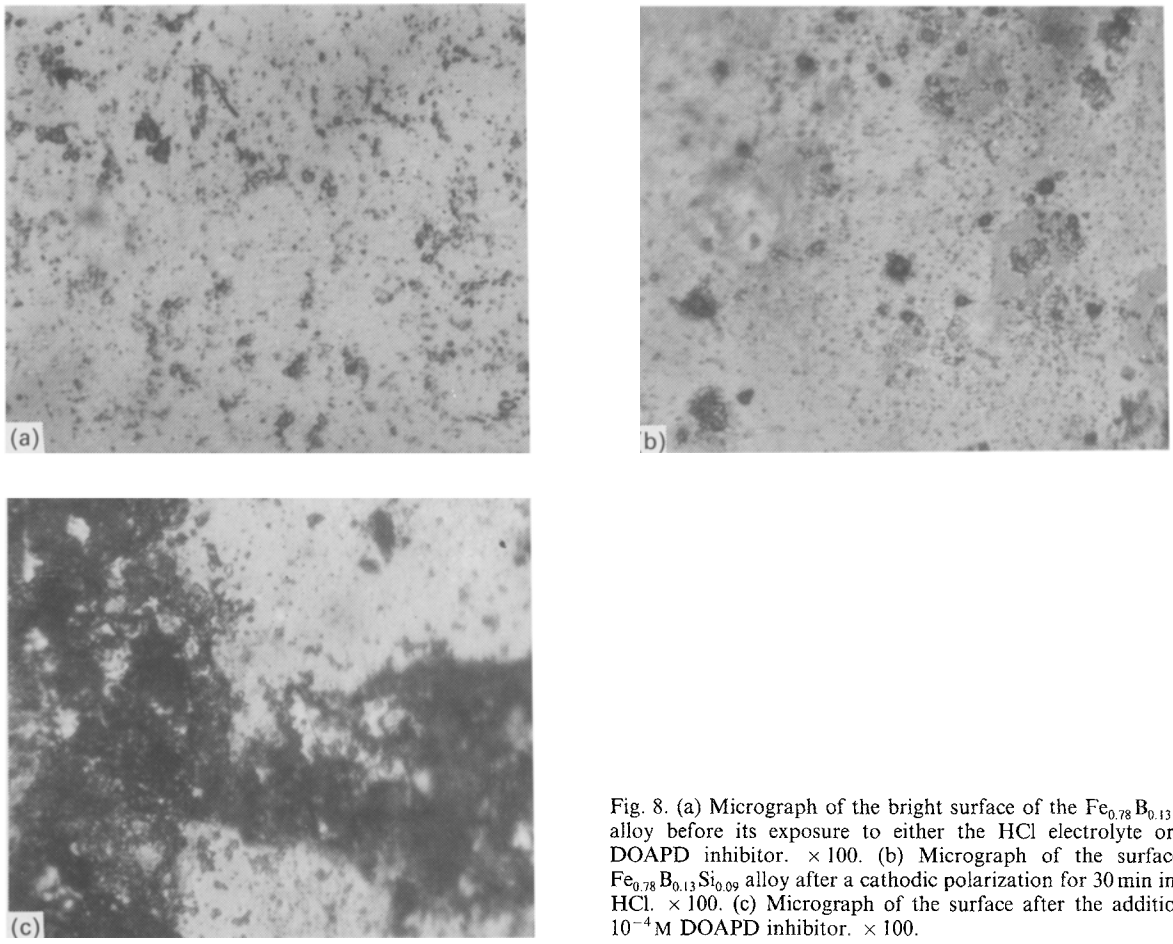

Fig. 8. (a) Micrograph of the bright surface of the $Fe_{0.78}B_{0.13}Si_{0.09}$ alloy before its exposure to either the HCl electrolyte or the DOAPD inhibitor. × 100. (b) Micrograph of the surface of $Fe_{0.78}B_{0.13}Si_{0.09}$ alloy after a cathodic polarization for 30 min in 1 M HCl. × 100. (c) Micrograph of the surface after the addition of 10^{-4} M DOAPD inhibitor. × 100.

immersed in 100 cm^3 of 1 M HCl at 19 ± 1° C. Complete dissolution of the alloy was observed after 12 h.

The weight loss of the alloy after the first hour of immersion was insignificant, which is why the weight was only recorded after 4 h of immersion.

The results of weight loss and inhibition efficiency as a function of DOAPD concentration are presented in Table 2. The efficiency is expressed by

$$e = \frac{w - w'}{w} \times 100$$

where w and w' are weight losses in the absence and presence of the inhibitor, respectively.

A comparison of the results presented in Tables 1 and 2 shows that corrosion occurs not only chemically but also by an electrochemical mechanism. The differences between the results in Tables 1 and 2 for each concentration could be attributed to pure residual chemical corrosion. These results confirm a good correlation between the two kinds of measurements.

The efficiency of different concentrations of the DOAPD inhibitor by the weight loss method is demonstrated in Fig. 6b. In this case, the adsorption could be treated in terms of an indirect adsorption Langmuir isotherm (Fig. 7).

Results obtained by electrochemical and gravimetric methods are in quite reasonable agreement and the following conclusions can be drawn.

(i) Maximum corrosion inhibition of the amorphous alloy studied is attained with DOAPD at 10^{-4} M (Fig. 6).

(ii) The indirect adsorption of DOAPD on the amorphous alloy corresponds to a Langmuir isotherm model in the concentration range below 10^{-4} M. The same maximum inhibition with DOAPD at 10^{-4} M is noted independently of the observation technique (gravimetric or electrochemical). It is important to note that the inhibition at concentrations higher than 10^{-4} M estimated from the electrochemical measurements is higher than that estimated from gravimetric technique. With the hypothesis that the decrease in both cases of the inhibition is attributed to the reduction of the inhibitor itself, one should not expect absolute parallelism between gravimetric and electrochemical results in the concentration range between 10^{-4} and 10^{-2} M. However, we are not able to confirm the absence of the reduction of the inhibitor although the observed characteristics (Fig. 7) seem inconsistent with electrochemical reduction of the inhibitor for the following reasons: (a) an increase in the corrosion current might be expected at all concentrations for the electrochemical measurement if the reduction product were desorbed; (b) if the reduction product were adsorbed, inhibition would continuously increase and electrochemical results would increase with all concentrations of DOAPD.

7. Inhibition of hydrogen surface embrittlement

As far as hydrogen surface embrittlement is concerned, optical observation of the surface of the amorph after being cathodically charged in 1 M HCl in the presence of the inhibitor compound clearly showed a diminution in superficial hydrogen blisters (see Fig. 8c). This conclusion is confirmed by comparing the cathodically charged amorphous surface state in 10^{-4} M DOAPD with the state in base electrolyte.

Comparing micrograph 8a (as reference) and micrograph 8b (for a charged alloy surface in the absence of the inhibitor), numerous blisters are observed due to hydrogen penetration into the alloy. Micrograph 8c in the presence of the inhibitor DOAPD shows that the number of hydrogen blisters on the charged amorphous surface has been markedly reduced. All these results demonstrate that this inhibitor is a mixed one and could be used not only as corrosion inhibitor but also in order to suppress hydrogen embrittlement.

8. Inhibition mechanism of DOAPD

We believe that the mechanism proposed earlier [23], explaining the double inhibition action of DOAPD on the corrosion and hydrogen penetration in crystalline α-iron, is valid for the amorphous $Fe_{0.78}B_{0.13}Si_{0.09}$ alloy treated in the present work. In the following we will briefly discuss this mechanism.

An inhibitor molecule is adsorbed on the metallic surface by means of the free electron pairs on the sulphur and the π electrons of the aromatic nuclei. This adsorption will certainly lead to an inhibition of metal dissolution. The amino groups of the adsorbed molecules trap the protons from the surrounding acid medium and prevent their reduction on the metallic surface. This may contribute to an increase in the hydrogen overpotential, reducing the amount of hydrogen available for penetration into the amorphous metal.

9. Conclusion

The results obtained in this work show clearly that the amorphous alloy $Fe_{0.78}B_{0.13}Si_{0.09}$ has a very weak corrosion resistance and is embrittled by hydrogen. DOAPD behaves as an effective mixed corrosion inhibitor for this amorph in 1 M HCl.

Potentiodynamic studies on $Fe_{0.78}B_{0.13}Si_{0.09}$ amorphous alloy in 1 M HCl showed that the addition of DOAPD to the electrolyte is accompanied by a strong decrease in the corrosion current density and an increase of the corrosion potential.

The inhibition efficiency of DOAPD in 1 M HCl deaerated solution was determined by a potentiodynamic study (Tafel line extrapolation) and by gravimetric weight loss methods. The inhibition efficiency increases with the increase of inhibitor concentration and attains a maximum value at 10^{-4} M DOAPD. The indirect adsorption of DOAPD (below 10^{-4} M) on the amorphous $Fe_{0.78}B_{0.13}Si_{0.09}$ alloy surface corresponds to the Langmuir isotherm model. Optical micrograph studies of $Fe_{0.78}B_{0.13}Si_{0.09}$ charged with hydrogen in the absence and presence of the DOAPD showed that the inhibitor significantly reduces the reactions between hydrogen and the amorphous surface.

Acknowledgements

The authors are very indebted to Drs J. Clavilier, B. Fotouhi and R. Reeves for fruitful criticisms and constructive comments, to Mr B. de Guillebon for generously donating the amorphous alloy. Dr A. Elkholy appreciates the permission of Dr M. Costa, Director of 'Laboratoire d'Electrochimie Interfaciale du C.N.R.S.', to work on a Post-Doctoral three months period with Dr M. Etman; Technical help by Mrs M. Doute, Mr H. Martin and Mr C. Mathieu is greatly appreciated.

References

[1] P. Duwez and S. C. H. Lin, *J. Appl. Phys.* **38** (1967) 4096.
[2] H. Jouve and G. Nicolas, 21e Colloque de Métallurgie INSTN-CEN, Saclay, France, Juin (1978) p. 437.
[3] G. J. Sellers, 'Metglass alloys an answer to low frequency magnetic sheilding', European EMC, Symposium, Montreux, Suisse, Juin (1977).
[4] W. Klement, R. H. Willens and P. Duwez, *Nature* **187** (1960) 869.
[5] T. Masumoto and H. Kimura, *J. Japan Inst. Metals* **39** (1975) 133.
[6] C. A. Pampillo, *J. Mat. Sci.* **10** (1975) 1194.
[7] T. Masumoto and R. Maddier, *Acta. Met.* **19** (1971) 725.
[8] A. Yokoyama, H. Komiyama, H. Inove, T. Masumoto and H. M. Kimura, *J. Catalysis* **68** (1981) 355.
[9] A. Yokoyama, H. Komiyama, H. Inove, T. Masumoto and H. M. Kimura, Proc. 4th Int. Conf. on 'Rapidly Quenched Metals' (1981); T. Masumoto and K. Suzuki (Eds), The Japan Institute of Metals, Sandai, Japan, Vol. II (1982) p. 1419.
[10] K. Hashimoto, M. Kasaya, K. Asami and T. Masumoto, *Corros. Sci.* **19** (1979) 857.
[11] M. Hara, K. Hashimoto and T. Masumoto, *J. Appl. Electrochem.* **13** (1983) 295.
[12] M. Naka and K. Hashimoto, *Corrosion* **32** (1976) 146.
[13] M. Naka, K. Hashimoto and T. Masumoto, *Corrosion* **36** (1980) 679.
[14] P. Cadet, M. Keddam and H. Takenouti, Fourth International Conference on 'Rapidly Quenched Metals', Sandai, Japan (1981).
[15] M. Naka, K. Hashimoto, A. Inove and T. Masumoto, *J. Noncryst. Solids* **31** (1979) 347.
[16] T. Masumoto and K. Hashimoto, 4th Int. Conf. on 'Liquid and Amorphous Metals', Grenoble, France (1980).
[17] M. da Conha Belo, B. Bondot and E. Navarro, *Mét. Corros. Ind.* **658** (1980) 2.
[18] J. P. Crousier, J. Crousier, Y. Massiani and C. Antonione, *Gaz. Chim. Ital.* **113** (1983) 329.
[19] T. Masumoto and H. Kimura, *Sci. Rep. Res. Inst., Tohuku Univ., Japan* **A27** (1979) 172.
[20] K. Belmokre, Doctorat de 3e Cycle, Marseille, France (1984).
[21] J. Czachor, *J. Electrochem. Soc.* **132** (1985) 306.
[22] A. Ben-Bachir, A. Sghiri, K. Ben-Chekroun and A. Elkholy, Int. Conf. on Corrosion Inhibition, Dallas, Texas, USA, May (1983).
[23] A. Elkholy, A. Ben-Bachir and K. Ben-Chekroun, The First Arabian Conference on Corrosion, Kowait, February 1984, Pergamon Press, London (1986) p. 310.
[24] B. de Guillebon, Third International Symposium on Developments in FRC Composites, Sheffield, England, July (1986).

[25] B. Donnely, T. C. Dowine, R. Grzeskowiak, H. B. Humburg and D. Short, *Corros. Sci.* **14** (1974) 597.
[26] B. Donnely, T. C. Dowine, R. Grzeskowiak, H. B. Humburg and D. Short, *Corros. Sci.* **18** (1978) 109.
[27] L. O. Riggs and R. L. Every, *Corrosion* **18** (1962) 262.
[28] K. Kobayashi and K. Ishli, 5th European Symposium on Corrosion Inhibitors, Ferrara, Italy (1980).
[29] K. C. Pillai and R. Narayan, *J. Electrochem. Soc.* **125** (1978) 1393.
[30] E. Blomgren and J. O'M. Bockris, *J. Phys. Chem.* **63** (1959) 1475.
[31] K. Ben-Chekroun, A. Ben-Bachir and A. Elkholy, 6th Symposium on Corrosion Inhibitors, Ferrara, Italy, September (1985).